# Molecular Depth Profiling Using a $C_{60}$ Cluster Beam: The Role of Impact Energy

**Andreas Wucher,[†] Juan Cheng,[‡,§] and Nicholas Winograd*[,‡]**

*Department of Chemistry, Pennsylvania State University, 104 Chemistry Building, University Park, Pennsylvania 16802, and Fachbereich Physik, Universität Duisburg-Essen, 47048 Duisburg, Germany*

*Received: June 5, 2008*

Molecular depth profiling of organic overlayers was performed using a mass-selected $C_{60}$ ion beam in conjunction with time-of-flight (TOF-SIMS) mass spectrometry. The characteristics of sputter depth profiles acquired for a 300-nm Trehalose film on silicon were studied as a function of the kinetic impact energy of the projectile ions. The results are interpreted in terms of a simple model describing the balance between sputter erosion and ion-induced chemical damage. It is shown that the efficiency of the projectile to clean up the fragmentation debris produced by its own impact represents a key parameter governing the success of molecular depth profile analysis.

## 1. Introduction

The latest advancement of cluster ion sources in secondary ion mass spectrometry (SIMS) instrumentation has opened new opportunities for materials characterization.[1,2] In particular, sputter depth profiling of molecular systems is now feasible,[3−12] a task which has been elusive because of the accumulation of ion beam-induced chemical damage.[13] Recently, several groups have demonstrated that the use of $C_{60}^+$ cluster projectile ions allows erosion of material while retaining molecular information in the mass spectra.[4,11,14−16] This observation opens the possibility of characterizing molecular solids below the surface and of elucidating the structure of buried interfaces in more complex systems.[2,14,17] An important goal is to combine molecular depth profiling with imaging using highly focused beam probes in order to acquire three-dimensional molecule-specific information.[6,18]

As the new properties of cluster SIMS emerge, it is important to understand the sputtering process from a physical point of view. A key to studying the interactions of energetic cluster ions with molecular solids is to begin with smooth and uniform thin films. We have recently established a well-defined, reproducible platform for investigating molecular depth profiling mechanisms which utilizes a thin film of trehalose sugar deposited onto a Si substrate.[19] The results obtained on these films have demonstrated the feasibility of molecular depth profiling, even in cases where the trehalose film is doped with different peptide molecules.[5,19,20] In order to understand the reason behind the success of cluster projectiles compared to atomic ions of the same impact energy, an analytical model was developed describing the erosion dynamics under irradiation of a molecular solid with energetic projectiles.[5,21] This model, although simplified, has been shown to provide a good fit to experimental depth profile data measured under irradiation with $C_{60}^+$, $Au_2^+$, and $Au_3^+$ cluster ions. It contains several empirical parameters describing the competition between ion beam-induced damage and removal of material from the surface.

In the present paper, we extend these studies by investigating the influence of the kinetic impact energy of the $C_{60}$ projectiles on these parameters over the range of 20 to 120 keV. The goal of this and related work[22,23] is to find optimum conditions which minimize the damage and make most efficient use of the sputtered material. In this respect, an efficiency parameter is introduced which describes the suitability of a projectile along with its impact conditions for successful molecular depth profile analysis. Our results show that impact energies of 20 − 40 keV provide the highest depth resolution of about 18 nm, along with the highest cleanup efficiencies.

## 2. Experimental Section

The experiments were performed using a time-of-flight (TOF) SIMS described in detail elsewhere.[24] The instrument is equipped with a fullerene ion source delivering a beam of mass-selected $C_{60}$ ions (Ionoptika C60−40). The projectile ions can be accelerated by up to 40 kV, mass selected by means of a Wien filter and focused into a spot size of less than 1 $\mu$m. The design of the source allows the extraction of ions in different charge states, thereby expanding the range of available kinetic impact energy up to 120 keV.

Preparation of the trehalose films has been described elsewhere.[4] Briefly, a 1 M aqueous trehalose solution was spin-cast onto a presliced 5 mm × 5 mm silicon wafer spinning at ∼3200 rpm. This procedure results in a homogeneous glassy layer as evidenced by a uniform color associated with the optical interference pattern created within the film.

The amount of material removed from the surface during cluster bombardment was determined by measuring the volume of the eroded crater using a large-view (800 $\mu$m × 800 $\mu$m) AFM (Nanopics 2100, KLA-Tencor). Assuming the density of the film to be equal to that of bulk trehalose (1.54 g/cm$^3$), the projectile ion fluence used to produce the crater can then be converted into the sputtering yield defined as the average number of trehalose molecule equivalents removed per incident projectile. If the crater extends into the Si substrate, it is necessary to account for the different sputtering rates of Si and trehalose. This correction is accomplished using a linear interpolation as

$$\dot{z}(t) = c_{\mathrm{Tre}}(t)\dot{z}_{\mathrm{Tre}} + c_{\mathrm{Si}}(t)\dot{z}_{\mathrm{Si}} \qquad (1)$$

where $\dot{z}(t)$ is the fluence dependent erosion rate, typically expressed in units of nm/s. Here, the weighting factors $c_{\mathrm{Tre}}(t)$

* Address correspondence to this author: E-mail: nxw@psu.edu.
† Universität Duisburg-Essen.
‡ Pennsylvania State University.
§ Current address: Merck & Co., Inc., WP78-210, 770 Sumneytown Pike, West Point, PA, 19486.

10.1021/jp8049763 CCC: $40.75 
Published on Web 09/27/2008

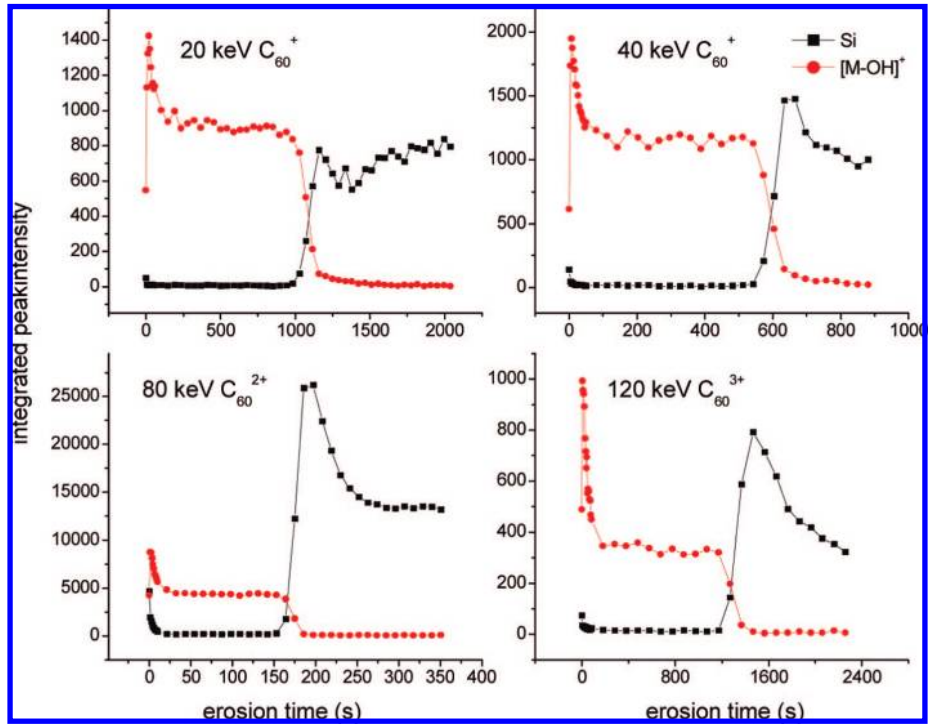


**Figure 1.** Raw data of trehalose $(M - OH)^+$ molecular ion signal and $Si^+$ substrate signal vs ion erosion time for different profiles taken with $C_{60}$ ions of different charge states and impact energies.

and $c_{Si}(t)$ are determined directly from the measured SIMS signals, $S_{Tre}$ and $S_{Si}$ representing the trehalose film and the silicon substrate, respectively, as

$$c_{Tre}(t) = \frac{S_{Tre}(t)/S_{Tre}^{max}}{S_{Tre}(t)/S_{Tre}^{max} + S_{Si}(t)/S_{Si}^{max}}$$

and

$$c_{Si}(t) = \frac{S_{Si}(t)/S_{Si}^{max}}{S_{Tre}(t)/S_{Tre}^{max} + S_{Si}(t)/S_{Si}^{max}} \quad (2)$$

The quantities $S_{Tre}^{max}$ and $S_{Si}^{max}$ denote the maximum value of the respective ion signal observed during the entire depth profile.

## 3. Results and Discussion

**3.1. Depth Profiles.** Examples of the uncorrected depth profiles for the $(M - OH)^+$ molecular ion signal of trehalose ($m/z$ 325) and the $Si^+$ substrate signal ($m/z$ 28) as a function of ion erosion time are shown in Figure 1. Using the Wien filter, different charge states of the $C_{60}$ projectile ions were selected for two different values of the ion acceleration voltage. In this way, kinetic impact energies of 20, 40, 80, and 120 keV could be achieved.

All profiles exhibit the characteristic features observed in our earlier work.[4,5,19] A very fast initial rise of the molecular ion signal is followed by a transient, where the signal falls exponentially toward a steady-state value. This value is then maintained throughout the complete removal of the overlayer. When the Si substrate is reached, the trehalose signal falls rapidly toward zero, while the Si signal rises accordingly. The $Si^+$ signal reaches a maximum value and then falls off toward a steady state signal characteristic of the pure Si substrate. We attribute the presence of this interface maximum to an enhanced ionization of the sputtered Si atoms due to the presence of oxygen-containing remnants of the organic overlayer.

Using the measured total crater depth, the erosion rate during the removal of the trehalose overlayer can be determined. Since all depth profiles are acquired by removing the entire trehalose film as well as part of the Si substrate, variation of the erosion rate between overlayer and substrate must be taken into account. For this purpose, Si erosion rates are estimated by

$$\dot{z} = \frac{\dot{f} Y^{tot}}{n} \quad (3)$$

assuming sputter yields $Y^{tot}$ of approximately 100, 200, 400, and 600 Si atoms removed per $C_{60}$ impact at 20, 40, 80, and 120 keV, respectively. These values are estimated by eroding craters into pure Si and by determining the amount of material removed for a specific primary ion fluence. In eq 3, $\dot{f}$ denotes the projectile ion flux density, and $n$ is the atom number density of the sample (50 atoms/nm$^3$ for Si). The erosion rate in the overlayer is determined by integrating eq 1 over the entire erosion time, setting the integral equal to the measured total crater depth and solving for $\dot{z}_{Tre}$. The resulting values are converted into trehalose sputter yields by means of eq 3, now inserting the trehalose number density (2.7 molecules/nm$^3$) for $n$ and integrating up to the erosion time where the interface is reached. The latter, in turn, is identified as the time when the trehalose signal has fallen to half of its steady state value.

The resulting values of the trehalose sputter yield vs the $C_{60}$ ion impact energy are listed in Table 1. The yield depends linearly on kinetic impact energy, the slope being 10.7 trehalose molecule equivalents (or 3660 amu) removed per ion impact and per keV of impact energy. A similar linear relation has been observed in experiments of $C_{60}$ and $Au_3$ bombardment of water ice.[25] These results have been interpreted in terms of a fluid dynamics model[25,26] in which the projectile energy is deposited in a track and the effected material arises from a conical volume that depends upon the cube of the track cylinder times the amount of energy deposited in a depth equal to the cylinder

**TABLE 1: Measured Interface Width Determined from the 84−16% Drop of the Trehalose $(M - OH)^+$ Molecular Ion Signal and Total Sputter Yield (in number of trehalose molecular equivalents removed per projectile impact) for Different Impact Energies and Charge States of the $C_{60}$ Projectile Ions**

| impact energy (charge state) | 20 keV (+) | 40 keV (2+) | 40 keV (+) | 80 keV (2+) | 120 keV (3+) |
|---|---|---|---|---|---|
| sputter yield (Tre/$C_{60}$) | 235 | 482 | 427 | 850 | 1260 |
| interface width (nm) | 18.3 | 17.6 | 18.3 | 20.7 | 22.5 |

radius. Simulations show that the cylinder radius is nearly independent of incident energy and that $C_{60}$ deposits its energy in an optimal depth in organic substrates for efficient removal of material.[25,27] Thus, the yield varies nearly linearly with incident kinetic energy. In fact, one can infer that the yield should be similar for all organic molecules as has been recently tabulated.[28]

With erosion rates determined, the time axis of Figure 1 can be replaced with a depth scale by integration of eq 1. The resulting depth profiles are depicted in Figure 2. Note that there is almost no erosion into the Si substrate, making the accuracy of the assumed Si sputter yields relatively unimportant. From Figure 2, the apparent depth resolution can be assessed by evaluating the distance between the points where the trehalose signal has fallen to 84% and 16% of its steady state value, respectively. The resulting interface width is depicted in Table 1. The depth resolution exhibits a slight degradation with increasing projectile impact energy, a finding which is quite common in sputter depth profiling experiments. For 20 keV, the absolute value of 18 nm listed here is slightly higher than our previously published value of about 12 nm,[19] which, however, had been determined using the 80−20% boundaries to define the transition.

**3.2. Erosion Dynamics.** As demonstrated previously,[5] the essential features of the profiles shown in Figure 1 can be explained in terms of a simple model describing the balance between ion-induced erosion and chemical damage. Briefly, it is assumed that a layer of thickness $d$ beneath the surface is modified by the projectile impact. In this layer, the concentration of intact analyte molecules is altered by three different fluxes, namely (i) the flux of material sputtered from the surface, (ii) the flux of molecules removed because of ion-induced chemical damage, and (iii) the flux of fresh, intact molecules that is exposed from the bulk because of the recession of the surface. As shown in detail elsewhere,[5,21] the resulting variation of the molecular ion signal is expected to vary with projectile ion fluence $f$ as

$$S(f) = S_{ss} + (S_0 - S_{ss})\exp[-(Y^{tot}/nd + \sigma_D)f] \qquad (4)$$

where $\sigma_D$ denotes the damage cross-section. For our model, $\sigma_D$ is the surface area in which analyte molecules are destroyed throughout the entire depth of the altered layer as a consequence of a single ion impact. As noted above, $Y^{tot}$ is the total sputter yield (in molecule equivalents removed per projectile impact) and $n$ is the sample density (in molecules per $nm^3$). The observed signal drops from a starting value $S_0$ to a steady-state value $S_{ss}$ determined by

$$S_{ss} = S_0 \frac{Y^{tot}}{Y^{tot} + nd\sigma_D} \qquad (5)$$

There is an initial increase in the secondary ion signal, not predicted by the erosion dynamics model, which we tentatively attribute to a varying ionization probability during the very early stages of the depth profile. It has been proposed that the $C_{60}$ projectile is effective at producing protons that quickly build up in the surface region and enhance the ionization via formation of $[M + H]^+$ species.[2,29,30] To accommodate this effect, it is necessary to begin the data analysis after the secondary ion signal begins to decay. By using eq 4 to fit this part of the curve

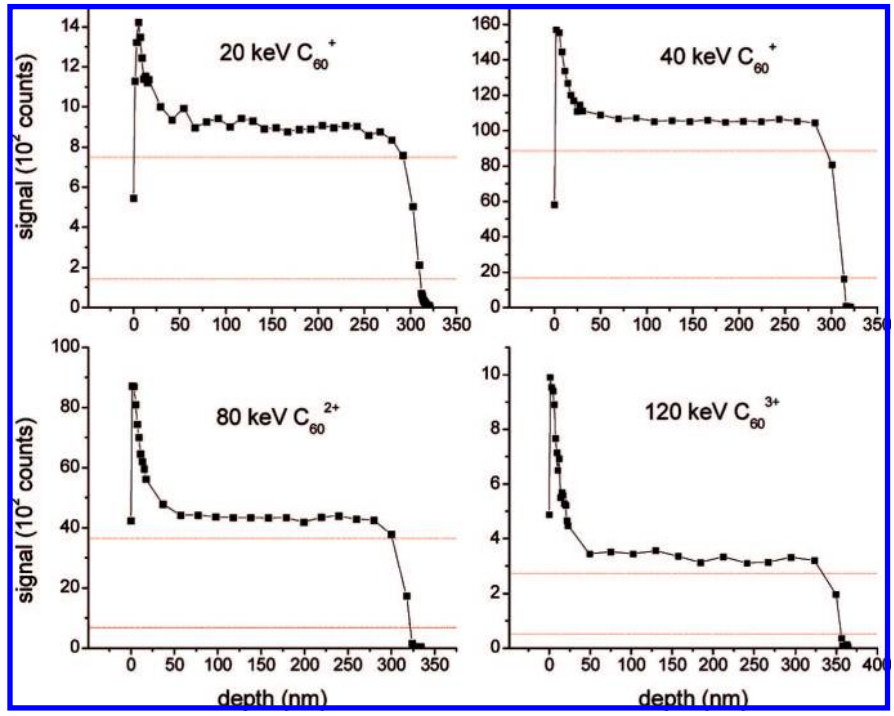


**Figure 2.** Depth profiles of trehalose $(M - OH)^+$ molecular ion signal at 325 amu for different impact energies of the $C_{60}$ projectile ions.

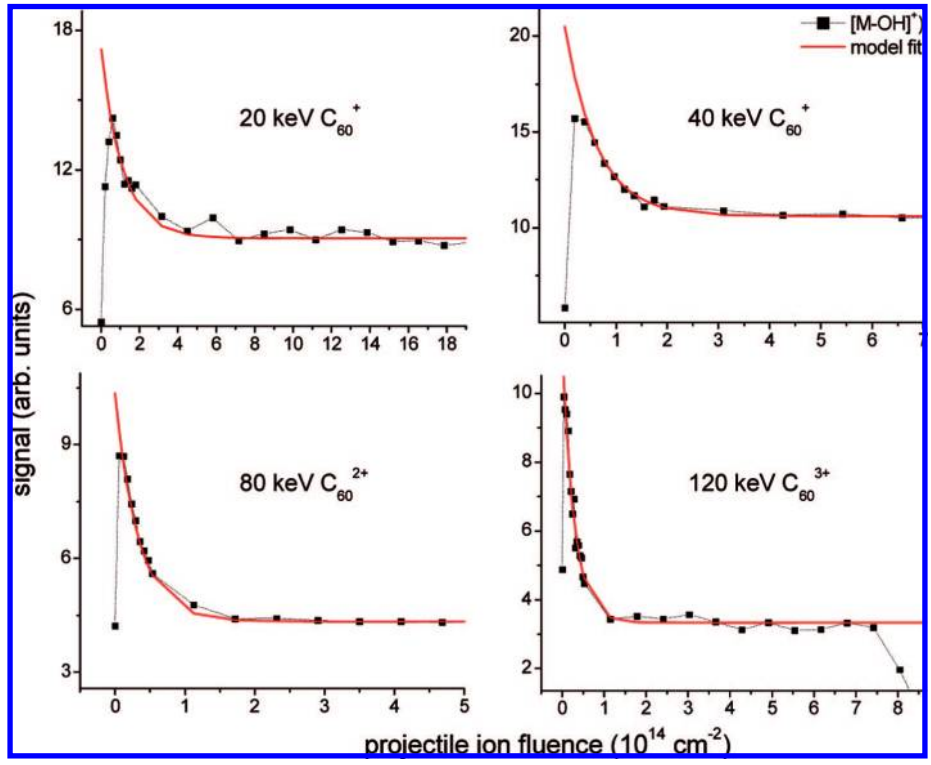


**Figure 3.** Fit of the erosion model described in the text (red curve) to the $C_{60}^{n+}$ ion fluence dependence of the $(M - OH)^+$ molecular ion of trehalose.

**TABLE 2: Altered Layer Depth ($d$) and Damage Cross-Section ($\sigma_D$), Signal Drop ($S_{ss}/S_0$) and Cleanup Efficiency ($\varepsilon$) Extracted from the Depth Profiles Shown in Figure 2 Using the Erosion Model Explained in the Text**

| impact energy (charge state) | 20 keV (+) | 40 keV (2+) | 40 keV (+) | 80 keV (2+) | 120 keV (3+) |
|---|---|---|---|---|---|
| $S_{ss}/S_0$ | 0.54 | 0.44 | 0.56 | 0.41 | 0.29 |
| $d$ (nm) | 23 | 24 | 23 | 32 | 40 |
| $\sigma_D$ (nm$^2$) | 3.3 | 9.6 | 5.6 | 14.5 | 34 |
| $\varepsilon$ | 1.18 | 0.78 | 1.30 | 0.70 | 0.41 |

to an exponential form, both the (virtual) starting signal $S_0$ and the disappearance cross-section $\sigma = (Y^{tot}/nd+\sigma_D)$ may be determined.

Examples of these fits are depicted in Figure 3. Using eq 5, the signal ratio $S_{ss}/S_0$ is then combined with the measured sputter yield to determine $d$ and $\sigma_D$ as the essential parameters describing the projectile−solid interaction. The resulting values are listed in Table 2 and are plotted vs impact energy in Figure 4. Both the altered layer depth and the damage cross-section clearly increase with increasing energy. Interestingly, the charge state of the projectile does not seem to influence the results outside the statistical reproducibility, suggesting that impact energy is the main parameter determining these values.

There is a convenient approach to quickly evaluate the quality of the depth profile using only the value of $S_{ss}/S_0$. As seen from eq 5, this ratio is determined by the relative magnitude of the number of sputtered molecules ($Y^{tot}$) in comparison to the number of molecules damaged per projectile impact, $nd\sigma_D$. In fact, one could define the ratio

$$\varepsilon = \frac{Y^{tot}}{nd\sigma_D} \tag{6}$$

as an efficiency parameter of a projectile for low-damage molecular depth profiling. The larger this ratio, the more of the debris produced by ion-induced fragmentation during one impact event will be removed in the same event. The process exposes fresh, undamaged analyte molecules which can be analyzed by a subsequent impact.

Combining eqs 5 and 6, one finds

$$\frac{S_{SS}}{S_0} = \frac{\varepsilon}{\varepsilon + 1} \tag{7}$$

thus allowing $\varepsilon$ to be determined from the signal drop at the beginning of the depth profile alone. The results are shown in Figure 5 and Table 2.

Although it appears as if there is a charge state dependence superimposed on the kinetic energy dependence of $\varepsilon$, it should be noted that the error bars denoting the reproducibility of the data are probably too large to reach a definitive conclusion regarding this point. Averaging all values determined for 40 keV, we find a monotonously decreasing cleanup efficiency $\varepsilon$ with increasing impact energy. This finding can be rationalized, since both $d$ and $\sigma_D$ increase faster with increasing impact energy than the sputter yield, thus making the cleanup less efficient.

A striking observation relates to the magnitude of the parameter $d$. At first sight, the values determined appear rather large. If the constituent atoms of the projectile were impinging independently, the mean range of a single C atom would vary between about 3 and 10 nm for total cluster impact energies between 20 and 120 keV. Apparently, the projectile cluster interacts with the solid as an entity before breaking up into its constituents, thus considerably enhancing the mean penetration

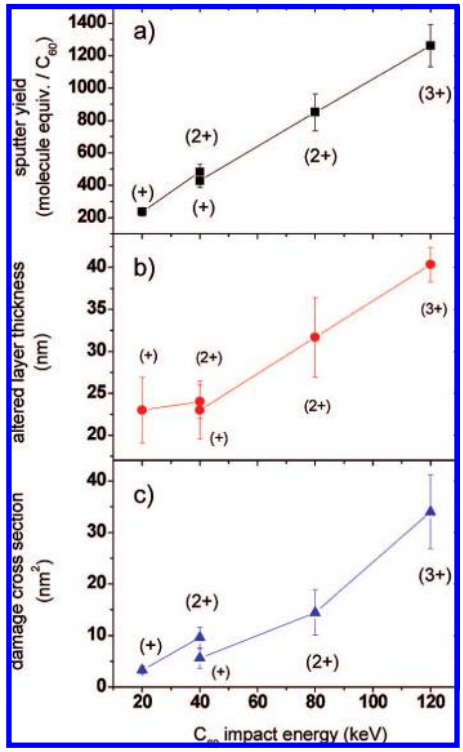


**Figure 4.** Total sputter yield (a), altered layer thickness (b) and damage cross-section (c) extracted from fitting of the erosion model to the measured depth profiles (see Figure 3) as a function of $C_{60}$ ion impact energy. The sputter yield values are given in molecular equivalents of trehalose removed per $C_{60}$ impact.

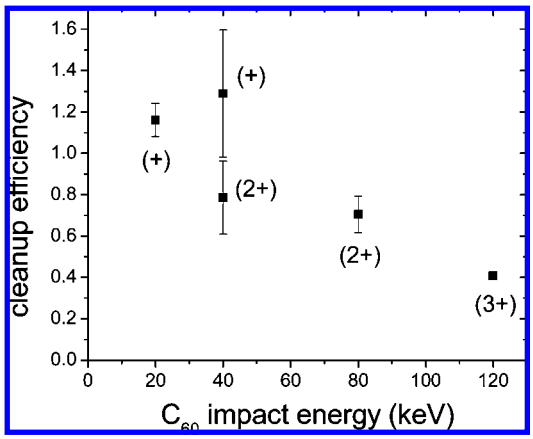


**Figure 5.** Cleanup efficiency parameter $\varepsilon$ as defined by eq 6) vs impact energy of $C_{60}^{n+}$ projectile ions.

range. This phenomenon has been reported earlier [31−33] and has been attributed to a "clearing the way" effect.[34,35]

On the other hand, there is an interesting relationship between the altered layer thickness and the measured width of the trehalose/silicon interface. As illustrated in Figure 6, the values of $d$ are significantly larger than the observed interface width. In fact, the difference between $d$ and the "intrinsic" depth resolution of the TOF-SIMS method is likely to be even larger, since the measured interface width is broadened by lateral inhomogeneities of the trehalose film thickness and/or the erosion rate.[36] Analysis of 3D depth profile data acquired on the same type of sample as investigated here has revealed an intrinsic depth resolution of about 8 nm under 40-keV $C_{60}$ bombardment,[36] thus suggesting that about 10 nm of all interface widths measured here may be assigned to such artifacts.

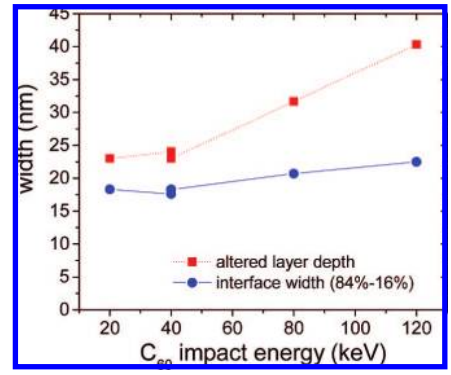


**Figure 6.** Altered layer depth extracted from erosion model fits (Figure 4b) and interface width measured in the depth profiles of Figure 2 vs impact energy of $C_{60}^{n+}$ projectile ions.

The apparent difference between altered layer depth and depth resolution can be rationalized as follows. In our model, the parameter $d$ is introduced to describe the average damage depth in a single projectile impact onto a bulk organic layer. The interface width, on the other hand, measures the information depth of the TOF-SIMS analysis method, which can in principle be influenced by (i) the depth interval from which the detected sputtered species originate and (ii) the range of ion beam-induced interlayer mixing effects. In a molecular depth profile of an organic film on a silicon substrate, one can assume the mixing contribution to be small, since it appears highly unlikely that an intact molecule can be mixed into the silicon substrate without being fragmented. Therefore, the "intrinsic" depth resolution basically reflects the depth of origin of sputtered intact molecules, which is certainly smaller than the damage depth and should be of the order of a few nanometers.[37]

## 4. Conclusions

By applying the erosion model to sputter depth profiles of trehalose films taken under $C_{60}$ cluster ion impact at different bombarding conditions, it is possible to extract valuable information about key quantities which characterize the efficiency of a projectile with respect to molecular depth profiling. As a first rule, it is found that the total sputter yield increases linearly with the kinetic impact energy. This behavior is also observed for other organic and inorganic samples and therefore seems to be a general characteristic of the sputtering process under energetic cluster bombardment. For trehalose, it is found that about 10 molecular equivalents or 3400 amu are removed per keV of $C_{60}$ impact. Interestingly, many $C_{60}$ sputter yield values published so far appear to be quite similar, covering a relatively narrow range from around 800 amu/keV for hard, metallic targets to about 3000 amu/keV for soft, organic, or ice films.

The thickness of the surface layer altered by the ion bombardment increases with increasing impact energy but appears to level off at values near 20 nm at the lowest energies investigated here. A similar but weaker trend is observed for the interface width. Interestingly, the depth resolution in these experiments is consistently found to be significantly better than suggested by the altered layer thickness, a finding which is understandable in view of the different information contained in both parameters. The damage cross-section is also found to increase with increasing impact energy, slightly stronger than linear. Combining all three effects, the efficiency of the cluster projectile to clean up the chemical damage generated by its own impact appears to be optimal for singly charged $C_{60}^{+}$ ions of

energies between 20−40 keV. Toward higher impact energies, both damage cross-section and altered layer thickness increase almost linearly, leading to a nearly quadratic energy dependence of their product as opposed to a linear increase of the sputter yield. As a consequence, the cleanup efficiency must decrease. Toward lower impact energy, on the other hand, the cleanup efficiency tends to become nearly constant, since the altered layer thickness becomes independent of energy.

**Acknowledgment.** Financial support from the National Institute of Health under grant no. EB002016-15, the National Science Foundation under grant no. CHE-055314, and the Department of Energy grant no. DE-FG02-06ER15803 are acknowledged.

## References and Notes

(1) Winograd, N. *Anal. Chem.* **2005**, *77*, 142A–149A.
(2) Wucher, A. *Appl. Surf. Sci.* **2006**.
(3) Gillen, G.; Simons, D. S.; Williams, P. *Anal. Chem.* **1990**, *62*, 2122–2130.
(4) Cheng, J.; Winograd, N. *Appl. Surf. Sci.* **2006**, *252*, 6498–6501.
(5) Cheng, J.; Wucher, A.; Winograd, N. *J. Phys. Chem. B* **2006**, *110*, 8329–8336.
(6) Fletcher, J. S.; Lockyer, N. P.; Vaidyanathan, S.; Vickerman, J. C. *Anal. Chem.* **2007**, *79*, 2199–2206.
(7) Mahoney, C.; Fahey, A.; Gillen, G. *Anal. Chem.* **2007**, *79*, 828–836.
(8) Mahoney, C.; Roberson, S.; Gillen, G. *Anal. Chem.* **2004**, *76*, 3199–3207.
(9) Sostarecz, A. G.; McQuaw, C. M.; Wucher, A.; Winograd, N. *Anal. Chem.* **2004**, *76*, 6651–6658.
(10) Wagner, M. S. *Anal. Chem.* **2005**, *77*, 911–922.
(11) Wucher, A.; Sun, S.; Szakal, C.; Winograd, N. *Anal. Chem.* **2004**, *76*, 7234–7242.
(12) Debois, D.; Brunelle, A; Laprevote, O. *Int. J. Mass Spectrom.* **2007**, *260*, 115–120.
(13) Benninghoven, A. *Surf. Sci.* **1994**, *299*, 246–260.
(14) Fletcher, J. S.; Conlan, X. A.; Lockyer, N.; Vickerman, J. C. *Appl. Surf. Sci.* **2006**, *252*, 6513–6516.
(15) Conlan, X. A.; Biddulph, G. X.; Lockyer, N. P.; Vickerman, J. C. *Appl. Surf. Sci.* **2006**, *252*, 6506–6508.
(16) Weibel, D. E.; Lockyer, N; Vickerman, J. C. *Appl. Surf. Sci.* **2004**, *231−232*, 146–152.
(17) Shard, A. G.; Green, F. M.; Brewer, P. J.; Seah, M. P.; Gilmore, I. S. *J. Phys. Chem. B* **2008**, *112*, 2596–2605.
(18) Wucher, A.; Cheng, J.; Winograd, N. *Anal. Chem.* **2007**, *79*, 5529–5539.
(19) Cheng, J.; Winograd, N. *Anal. Chem.* **2005**, *77*, 3651–3659.
(20) Wucher, A., Cheng, J.,Winograd, N. *Appl. Surf. Sci.* **2008**, in press.
(21) Wucher, A. *Surf. Interface Anal.* **2008**, in press.
(22) Kozole, J.; Wucher, A.; Winograd, N. *Anal. Chem.* **2008**, in press.
(23) Zheng, L. L., Wucher, A.,Winograd, N. *Anal. Chem.* **2008**, in press.
(24) Braun, R. M.; Blenkinsopp, P.; Mullock, S. J.; Corlett, C.; Willey, K. F.; Vickerman, J. C.; Winograd, N. *Rapid Commun. Mass Spectrom.* **1998**, *12*, 1246.
(25) Russo, M. F.; Szakal, C.; Kozole, J.; Winograd, N.; Garrison, B. J. *Anal. Chem.* **2007**, *79*, 4493–4498.
(26) Russo, M. F., Jr.; Garrison, B. J. *Anal. Chem.* **2006**, *78*, 7206–7210.
(27) Ryan, K. E. and Garrison, B. J. *Anal. Chem.* **2008**, in press.
(28) Delcorte, A.; Garrison, B. J. *J. Phys. Chem. C* **2007**, *111*, 15312–15324.
(29) Conlan, X. A.; Lockyer, N. P.; Vickerman, J. C. *Rapid Commun. Mass Spectrom.* **2006**, *20*, 1327–1334.
(30) Winograd, N.; Postawa, Z.; Cheng, J.; Szakal, C.; Kozole, J.; Garrison, B. J. *Appl. Surf. Sci.* **2006**, *252*, 6836–6843.
(31) Russo, M. F., Jr.; Wojciechowski, I.; Garrison, B. J. *Appl. Surf. Sci.* **2006**, *252*, 6423–6425.
(32) Smiley, E. J.; Winograd, N.; Garrison, B. J. *Anal. Chem.* **2007**, *79*, 494–499.
(33) Smiley, E. J.; Wojciechowski, I. A.; Postawa, Z.; Winograd, N.; Garrison, B. J. *Appl. Surf. Sci.* **2006**, *252*, 6436–6439.
(34) Sigmund, P.; Bitensky, I. S.; Jensen, J. *Nucl. Instrum. Methods B* **1996**, *112*, 1–11.
(35) Anders, C.; Urbassek, H. M. *Nucl. Instrum. Methods B* **2007**, *258*, 497–500.
(36) Wucher, A., Cheng, J., Zheng, L., Willingham, D.,Winograd, N. *Appl. Surf. Sci.* **2008**, in press.
(37) Szakal, C.; Kozole, J.; Russo, M. F., Jr.; Garrison, B. J; Winograd, N *Phys. Rev. Lett.* **2006**, *96*, 216104-1–216104-4.

JP8049763